Liquid film stability and contact line dynamics of emulsion liquid films in curtain coating process

Alireza Mohammad Karim [ID]**, Wieslaw J. Suszynski, Saswati Pujari**

Abstract Previous studies reported that single-phase liquid curtains become more stable with increasing Ohnesorge number. Many liquid films used in the coating industry are types of emulsion samples. Despite this fact, the effect of multiphase liquids on the dynamics of the curtain breakup has not yet been considered. This study explores the stability of emulsion curtain coating via high-speed visualization. The critical condition at the onset of curtain breakup was determined by finding the flow rate below which the curtain broke. Curtain breakup was observed via a hole initiation within the curtain. The results reveal that curtain breakup dynamics is governed by the characteristic dynamic viscosity and the surface tension. The emulsion curtain stability, defined by Weber number, increases as Ohnesorge number rises, similar to the single-phase liquid (i.e., Newtonian and pure shear thinning) curtain stability. The critical web speed at which the contact line moves upstream of the curtain, a phenomenon called heel formation, and that at which air entrainment occurs, were determined for emulsion solutions at different flow rates. The results reveal that the surface tension increase delays the onset of air entrainment which could help to conduct faster curtain coating substrates with emulsion liquid films.

Keywords Liquid film stability, Shear thinning, Multiphase liquid, Liquid contact line

A. Mohammad Karim (✉), W. J. Suszynski
Department of Chemical Engineering and Materials
Science, University of Minnesota, 421 Washington Ave. SE,
Minneapolis, MN 55455, USA
e-mail: alireza.m.k.2010@gmail.com

S. Pujari
Dow, 400 Arcola Road, Collegeville, PA 19426, USA

Introduction

Curtain coating is one of the preferred methods for high-speed precision coating of single-layer and multilayer films. In curtain coating, a liquid sheet forms as the liquid exits the coating die and flows freely downward before it impinges on the surface of the moving substrate to be coated, as sketched in Fig. 1a.[1–10] Curtain coating is challenging. A uniform thin liquid layer is only obtained within the limited range of operating parameters, as sketched in Fig. 1b,[1] usually referred to as the coating window. Figure 1b represents the operating space for curtain coating in terms of two dimensionless numbers: the ratio of the web speed, U_{web}, to the curtain velocity at the liquid contact line, U, and the Reynolds number, defined as $\mathrm{Re} = \frac{\rho Q}{\mu_0}$, where Q is the flow rate per unit width, ρ is the liquid density, and μ_0 is the liquid zero-shear viscosity.

To achieve a thinner coating, a lower flow rate out of the die and a thinner liquid curtain are needed. It is worthwhile to mention that for all premetered coating techniques, such as the curtain coating, the thickness of the coated liquid film, h_{film}, depends on the ratio of the flow rate per unit width, Q, and the substrate speed, U, via $h_{film} = Q/U$. As a result of this, increasing the substrate speed is also another way for achieving the thinner liquid coated films.[2] However, the liquid curtain breaks when the flow rate falls below a certain critical value. The instability of liquid sheet is a physical phenomenon that was studied first by Taylor in 1959.[11] Based on Taylor's analysis, Brown[12] presented the first experimental study on the stability of the liquid curtain exhibiting Newtonian behavior. He proposed a stability criterion considering the comparison of the inertial force in the liquid curtain, which pushes downward a hole created within the liquid curtain, with the capillary force, which causes the hole

to move upward. This stability criterion is therefore represented by the Weber number, We, which signifies the relative importance of inertial and capillary effects [equation (1)]:

$$\mathrm{We} = \frac{\rho Q U}{2\sigma} > 1 \qquad (1)$$

where Q is the flow rate per unit width of the liquid curtain, U is the liquid curtain velocity, ρ is the density of the liquid, and σ is the surface tension of the liquid.

Many scientists have investigated the validity of the Brown's stability criterion.[13–18] Several studies[8,16–21] have found conditions under which the critical parameters at the onset of curtain breakup are not well described by Brown's criterion. The mechanisms of liquid curtain breakup are more complex than the simple balance between inertial and capillary forces. The viscosity of the liquid may have an important effect on curtain stability. Experimental results reported by Karim et al.[4] and numerical analyses presented by Sünderhauf et al.[20] have shown that the viscosity increases the stability of the liquid curtain. Theoretical and numerical analyses presented by Savva and Bush[21] concluded the important effect of viscosity is on the growth rate of a hole formed within a liquid curtain. This behavior was confirmed with the experimental results from Karim et al.[4] This study[4] also revealed that the liquid viscosity affects Newtonian liquid curtain stability in two ways: (1) it slows down the retraction speed of the rim of a hole in the curtain, stabilizing it, and (2) it slows down the curtain speed inside the viscous boundary layer that is formed near the edge guides, promoting curtain breakup. With properly designed edge guides the first effect dominates.

Curtain coating process also relies on steady dynamic wetting to uniformly deposit a liquid film onto a moving web. Above a critical substrate speed, the air layer in contact with the substrate is not fully displaced, the flow evolves from steady two-dimensional to unsteady three-dimensional flow[22–24] and a small amount of air is entrained under the liquid layer. Air entrainment degrades film uniformity and product quality and therefore should always be avoided in coating processes.[25]

In curtain coating, the momentum of the liquid flowing down the curtain creates a high-pressure region near the contact line that helps displace the air layer in contact with the substrate, enabling wetting at higher speeds than observed in other coating methods.[26,27] The delay in air entrainment associated with this high-pressure region is generally referred to as "hydrodynamic assist."[1–3,28]

At each flow rate above the critical value, there is a range of web velocity at which two-dimensional flow occurs. If the web velocity is not high enough, liquid accumulates in the coating bead, the dynamic contact line moves upstream of the curtain, and the flow becomes nonuniform in the cross-web direction. This phenomenon is usually called heel formation. The maximum speed at each flow rate marks the onset of air entrainment. As sketched in Fig. 1b, experimental observations show that the degree of hydrodynamic assist reaches its maximum (i.e., the largest critical speed) at a specific flow rate, at which the dynamic contact line (DCL) is right beneath the liquid curtain, which leads to a strong hydrodynamic pressure near the DCL as the liquid impacts the substrate.[1,2,26,27,29–31]

Typical liquids used in curtain coating are complex colloidal suspensions or emulsions,[32] which exhibit shear thinning behavior. Despite the broad technological application of emulsion liquid films in the coating industry, there is still a lack of fundamental understanding of the importance of these multiphase liquids on curtain breakup mechanism and stability of the dynamic contact line. In this work, a comprehensive analysis of the relation between the physical properties of dilute emulsion solutions and curtain coating stability was presented.

Materials and methods

Experimental setup

The curtain coating setup is sketched in Fig. 2. A peristaltic pump delivers liquid from the tank to the coating die to form a curtain between two Teflon-coated edge guides at an angle of two degrees. The dynamics of the curtain breakage was recorded, and the local curtain velocity, u, at different positions (x, y) along the curtain, where x is the distance from the edge guide and y is the distance from the lip of the slide coating die, was also determined. Details of the experimental procedures are described in previous studies of liquid curtain stability.[4,5,8]

The dynamic contact line was monitored from the back and front of the curtain to observe air entrainment and heel formation at different flow rates and speeds of the glass roll as indicated in Fig. 2a. The curtain and deposited film were also recorded with a Canon camera mounted in front of the curtain with a field of view that spanned the width of the curtain; also, indicated in Fig. 2a.

At each constant flow rate, Q, the speed of the glass roller, U_w, was increased slowly until V-shape air pocket(s) were observed. The corresponding speed of the glass roller is defined as the critical speed for onset of air entrainment. For the same flow rate, the speed of the glass roller was then decreased slowly until a heel of liquid was observed at any location along the dynamic contact line. The corresponding speed of the glass roller is defined as the critical speed for onset of heel formation. The maximum speed, $U_{w,max}$, the glass roller can achieve in the experiment is 164.2 cm/s.

Figure 3 illustrates the visualization from back and front views of the dynamic contact line representing
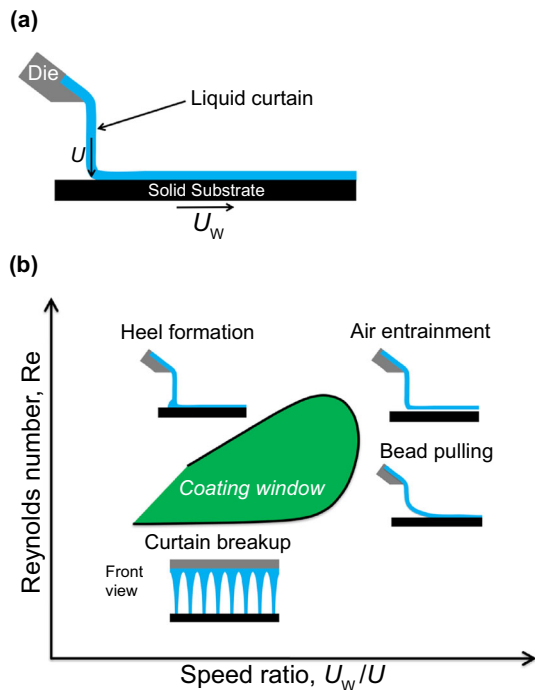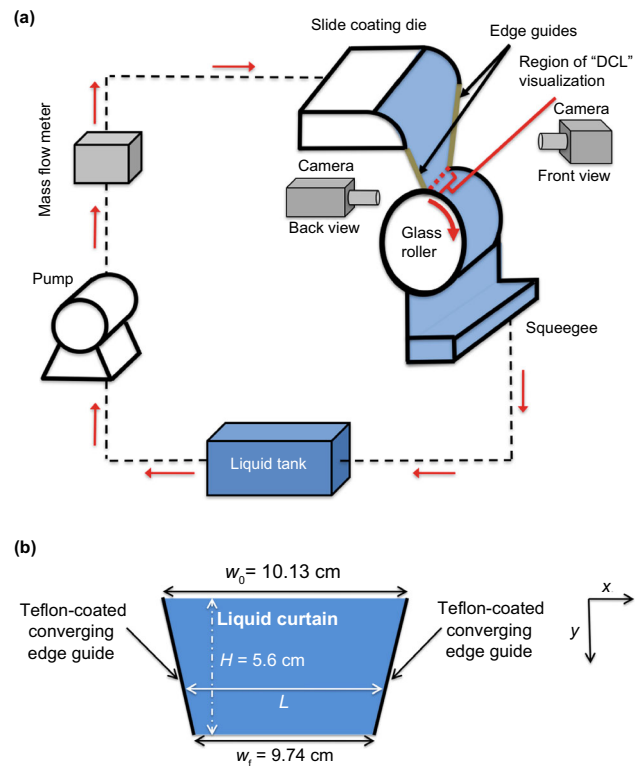
Fig. 1: (a) The schematic of a stable curtain at web speed, U_W, and curtain velocity at the impingement zone, U. (b) Schematic of curtain coating window[1]


Fig. 2: (a) Schematics of the curtain coating setup used in the experiments. Dotted lines with arrows indicate the direction of the liquid flow in the curtain coating setup. (b) Front view of the liquid curtain between two Teflon-coated converging (inclined) edge guides. **H** is the height of the curtain and **L** is the local width of the curtain

stable dynamic contact line, air entrainment, and heel formation for emulsion solution. The presence of V-shape air pockets along the dynamic contact line reveals air entrainment (see Fig. 3c). Heel formation is defined by the presence of excess liquid column along the dynamic contact line (see Fig. 3b). It is important to note that we decided to specify the onset of heel formation at the instance at which we observed the beginning of the liquid accumulation just behind the impingement zone where the stable dynamic contact line is defined, which is the location exactly underneath the falling emulsion liquid film vertically on the glass roller.

Materials

The acrylic emulsion used in this study was a typical water-based acrylic adhesive made by Dow. These emulsions have been thickened with rheology modifier available commercially from Dow. The shear viscosity curves were obtained using the AR-G2 Rheometer (TA Instruments) with a Couette cell geometry. In the range of shear rate explored, the viscosity curves show a low-shear plateau, a power-law region ($\mu = K\dot{\gamma}^{n-1}$, where μ is shear viscosity, $\dot{\gamma}$ is shear rate, K is flow consistency index, and n is flow behavior index) and a

high-shear plateau value. The emulsion samples used in this study exhibit shear thinning behavior (see Fig. 4).

The characteristic rate of deformation of the curtain breakup flow can be estimated by assuming a radial flow during the hole opening process in a free liquid sheet. It is given by the ratio of the rim velocity, u_{rim}, to the curtain width, L: $\dot{\gamma}^* = u_{rim}/L$. For the conditions of the present experiments (see next section), the characteristic deformation rate is approximately $\dot{\gamma}^* = 13.5 \text{ s}^{-1}$. The liquid characteristic dynamic viscosity at this characteristic shear rate is referred to as μ_C ($\mu_C = \mu(\dot{\gamma}^*)$).

Table 1 shows the physical properties of emulsion solutions prepared for the experiments. The surface tension was measured using the Wilhelmy plate method[33] in the digital tensiometer K10ST (Krüss), and density was determined by Krohne MFC 100 Coriolis-type mass flow meter used in curtain coating experiment.

(a) **(b)** **(c)**
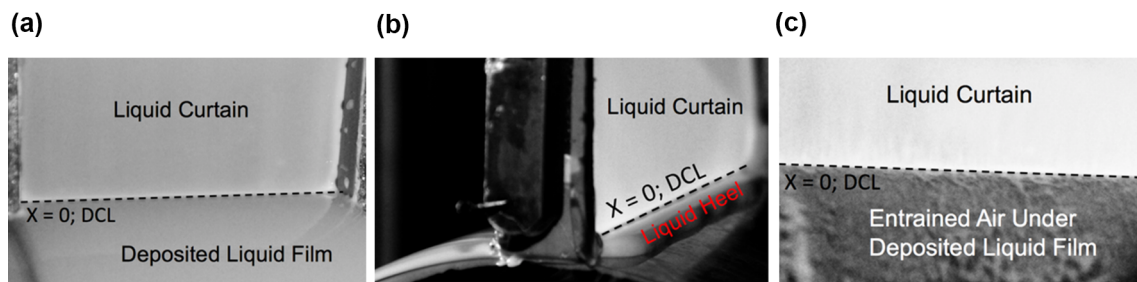
Fig. 3: (a) Stable dynamic contact line. (b) Heel formation along dynamic contact line. (c) Air entrainment along dynamic contact line
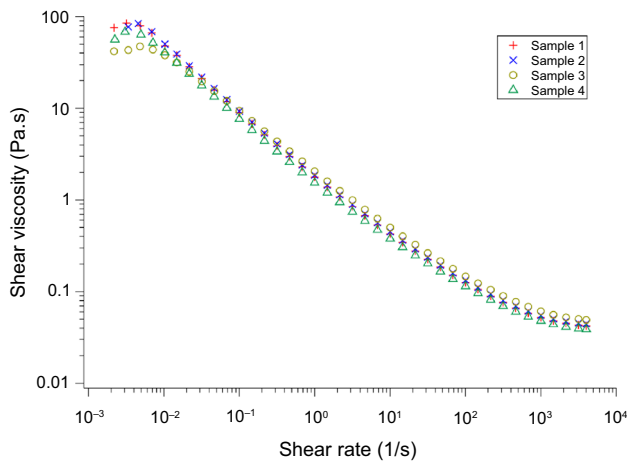
Fig. 4: Rheological characteristics of emulsion samples tested in this study

Results and discussion

Liquid velocity in the curtain

Since the stability condition for the liquid curtain is highly related to the ratio between the speed at which a disturbance (i.e., hole) expands in the curtain and the speed by which the hole is convected by flow, it is crucial to determine the effect of viscous forces on the liquid velocity in the curtain. The velocity of the liquid curtain at different distances from the edge guides was measured by tracking the downward motion of air bubbles, as shown in Fig. 5. The free fall velocity, U_g, is described by equation (2):

$$U_g = \left(U_{exit}^2 + 2gy\right)^{1/2} \qquad (2)$$

where y is the distance from the die, U_{exit} is the velocity on the top of the curtain, defined in a first approximation as $U_{exit} = \frac{Q}{h_{slot}}$, where Q is the volumetric flow rate per unit width of the die and h_{slot} is the slot height, which is 508 μm, and g is gravitational acceleration. The free fall velocity is illustrated in Fig. 5 as a dashed line.

The experiments were done using a slide-fed curtain coating die. Therefore, the velocity on the top of the

curtain needs to take into account the viscous forces along the flow down the inclined plane of the die and along the edge guides of the curtain. The film thickness h_{die} and velocity at the end of the incline U_{die} can be estimated by assuming a steady state, laminar, one-dimensional, fully developed, and incompressible flow of a power-law liquid on an inclined plane under the effect of gravity (the shear rates of the flow down an inclined plane are inside the power-law region of the viscosity curves) to solve the Navier–Stokes equation in the direction of flow, x^* [equation (3)]:[34–36]

$$\frac{d}{dy^*}\left(\tau_{x^*y^*}\right) + \rho g \sin \alpha = 0 \qquad (3a)$$

$$\tau_{x^*y^*} = K\left(\frac{du_{die}}{dy^*}\right)^{n-1}\frac{du_{die}}{dy^*} \qquad (3b)$$

where u_{die} is the velocity along the surface of the die and y^* is the axis vertical to the surface of the die and applying the boundary conditions on the flow along the surface of the die equation (4):

$$(u_{die})_{y^*=0} = 0 \,(\text{no-slip along the surface of the die}) \qquad (4a)$$

$$\left(\frac{du_{die}}{dy^*}\right)_{y^*=h_{die}} = 0 \,(\text{shear-free along the liquid-air interface}) \qquad (4b)$$

the relation between the flow rate per unit width and the liquid film thickness can be obtained using equation (5):

$$h_{die} = \left[\left(\frac{2n+1}{n}\right)\left(\frac{\rho g \sin \alpha}{K}\right)^{-1/n} Q\right]^{\frac{n}{2n+1}} \qquad (5a)$$

$$Q = \int_{y^*=0}^{y^*=h_{die}} u_{die}\,dy^* = h_{die}U_{die} \qquad (5b)$$

where Q is flow rate per unit width of the curtain, $\alpha = 60°$ is the inclination angle of the die surface, K is the

Table 1: The physical properties of emulsion solutions

Sample	Density ρ (kg/m^3)	Surface tension σ (mN/ m)	Shear viscosity at characteristic shear rate, μ_{10} (Pa.s)	Low-shear viscosity μ_0 (Pa.s)	High-shear viscosity μ_∞ (Pa.s)	K (Pa sn)	n
1	1007.5	41.9	0.4277	85.07	0.0425	1.5210	0.239
2	1007.3	36.9	0.4512	84.26	0.0446	1.6232	0.247
3	1007.5	33.3	0.5006	47.40	0.0491	2.1561	0.360
4	1007.6	52.8	0.3795	68.21	0.0388	1.3668	0.257
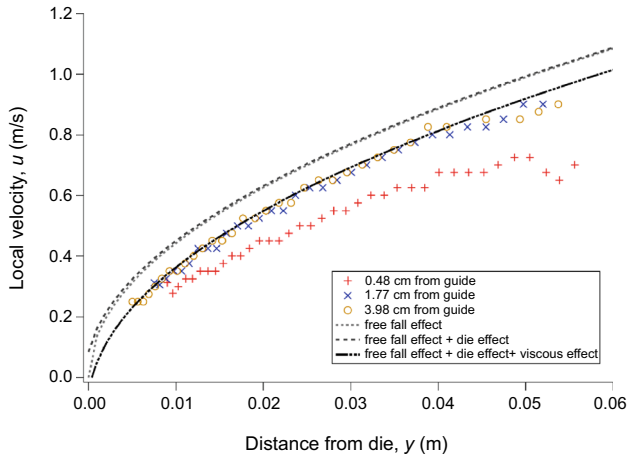
Fig. 5: The velocities of the air bubbles within the liquid curtain for sample 2. The measurement uncertainty in *u* and *y* is less than the size of the data points

flow consistency index, and n is flow behavior index. Hence, the velocity at the end of the inclined plane of the die can be determined by equation (6):

$$U_{\text{die}} = \left(\frac{n}{2n+1}\right)\left(\frac{\rho g \sin \alpha}{K}\right)^{1/n} h_{\text{die}}^{\left(\frac{n+1}{n}\right)} \tag{6}$$

The curtain velocity estimation considering the free fall effect as well as the viscous effect along the slide die surface, U_{gd}, is shown in the plots of Fig. 5 and is given by equation (7):

$$U_{\text{gd}} = \sqrt{U_{\text{die}}^2 + 2gy} \tag{7}$$

The velocity of the curtain is also affected by the viscous boundary layer that is formed along the edge guides. The velocity reduction associated with the boundary layer was estimated by Marston et al.[36] as shown in equation (8):

$$U_{\text{edge}} = \left[\frac{9\rho g(\cos \beta)Q^2}{8\mu(\dot{\gamma})}\right]^{1/3} \tag{8}$$

where $\mu(\dot{\gamma}) = K\dot{\gamma}^{n-1} = K\left(\frac{\mathrm{d}u_v}{\mathrm{d}y}\right)^{n-1}$ for $u_v = \left(U_{\text{die}}^2 + 2gy\right)^{1/2}$ and $\beta = 2°$ is the inclination angle (i.e., from vertical) of the converging edge guides used in the experiments reported here.

Therefore, the liquid velocity in the curtain, U, can be estimated via considering the viscous effects along the edge guides as well as the surface of the die in addition to the free fall effect [equation (9)]:

$$U = \sqrt{U_{\text{die}}^2 + 2gy} - U_{\text{edge}} \tag{9}$$

This plot of the velocity curve considering the viscous effects along both the edge guides and the surface of the die as well as the free fall effect is also shown in the plots illustrated in Fig. 5. For bubbles at different positions with respect to the edge guides, the measured velocity of the curtain is well described by equation (9) for liquid particles in the curtain located outside the viscous boundary layer, formed along the edge guides. Moreover, the velocity of the liquid curtain particles located near the edge guides is systematically lower than the velocity predicted by equation (9). This large velocity difference may be attributed to the strong and variable viscous effect within the viscous boundary layer formed along the edge guides (see Fig. 5).[34–36] It is important to note that the viscous effect along the slide die surface did not have a significant influence on the velocity of the liquid curtain particles as illustrated in Fig. 5.

Visualization of the liquid curtain breakup

High-speed visualization was used to analyze the sequence of events that leads to the liquid curtain breakup. Figure 6 shows the expansion of a hole formed within the curtain and the eventual complete breakup of the liquid curtain into individual liquid columns for sample 4. The entire process for complete curtain breakup took 181.5 ms. The breakup process is similar to the one for single-phase liquids.[4,8]
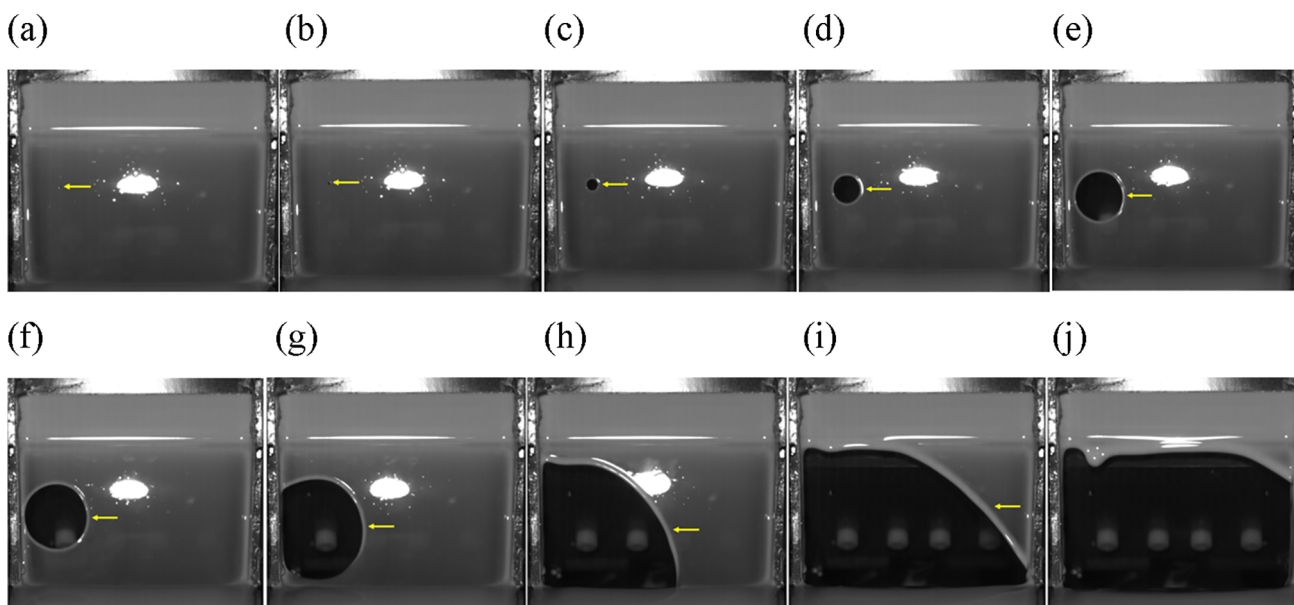
Fig. 6: The mechanism of the emulsion liquid curtain breakage for sample 4. (a) $t = 0$ ms. (b) $t = 0.5$ ms. (c) $t = 3$ ms. (d) $t = 7$ ms. (e) $t = 12$ ms. (f) $t = 15$ ms. (g) $t = 22$ ms. (h) $t = 44$ ms. (i) $t = 96.5$ ms. (j) $t = 181.5$ ms

Growth dynamics of hole within the emulsion liquid film

As illustrated in Fig. 6, liquid curtain breakup is initiated by the formation of a hole within the liquid curtain. The capillary force pulls the rim of the hole, causing expansion. At the same time, the curtain flow convects the hole downward. The dynamics of the hole expansion along the horizontal axis (i.e., along the width of the liquid curtain) and the vertical axis (i.e., along the height of the liquid curtain) was analyzed by measuring the evolution of the horizontal positions of right, x_R, and left, x_L, rims and the vertical positions of top, y_T, and bottom, y_B, rims during a hole expansion for different solutions, and the results are presented in Fig. 7.

The rim speeds in x-direction ($u_{x,L}$ and $u_{x,R}$), where $u_{x,L}$ and $u_{x,R}$ are the speeds at left and right sides of the hole, respectively, and y-direction ($u_{y,B}$ and $u_{y,T}$), where $u_{y,B}$ and $u_{y,T}$ are the speeds at bottom and top parts of the hole, respectively, were calculated from the data in Fig. 7, for the time interval of the hole expansion for each experiment before the complete curtain breakup. The measured retraction speeds obtained from different emulsion solutions are presented in Fig. 8a. The measured retraction speeds are normalized by the Taylor–Culick[11,37] rim speed, U_{TC}, defined as:

$$U_{TC} = \sqrt{\frac{2\sigma}{\rho t}} \quad (10)$$

In equation (10), t is the local film thickness at the position of the hole formation, which is evaluated based on the local curtain velocity and mass conservation:

$$t = \frac{q}{U_{Curtain} w_{Curtain}} \quad (11)$$

In equation (11), $w_{Curtain}$ is the local width of the curtain, q is the critical volumetric flow rate for curtain breakup, and $U_{Curtain}$ is the liquid curtain velocity at the location of hole initiation.

The plot presented in Fig. 8a represents both the horizontal and vertical rim speeds, as indicated in Fig. 8b, as a function of the Ohnesorge number, Oh, defined here in terms of the characteristic shear viscosity μ_C equation (12):

$$Oh = \frac{\mu_C}{\sqrt{2\rho\sigma t}} \quad (12)$$

Therefore, each liquid investigated has a unique Oh. Table 2 presents the initial location of the hole in the curtain and its bounding rim speeds for each solution tested. The curtain thickness at the breakup point, the corresponding Taylor–Culick speed, and Ohnesorge number are also presented.

It is important to note that the horizontal retraction speed is on the order of 1 m/s, the same order of magnitude as the curtain velocity at the location of the hole formation (see Table 2). This agrees well with the general stability criterion stating that the curtain becomes unstable if the retraction speed is equal to the curtain velocity. The measured horizontal retraction speed agrees well with the Taylor–Culick speed and falls within the Ohnesorge number defined in terms of the characteristic shear viscosity (see Fig. 8).
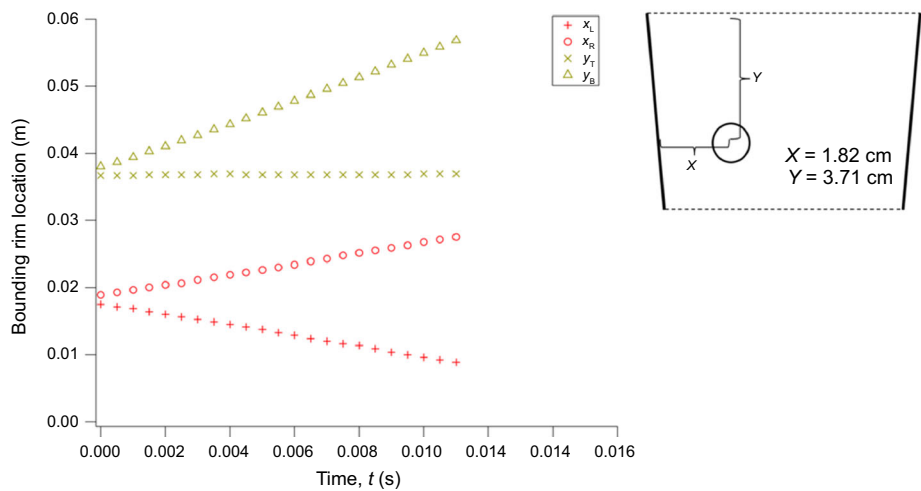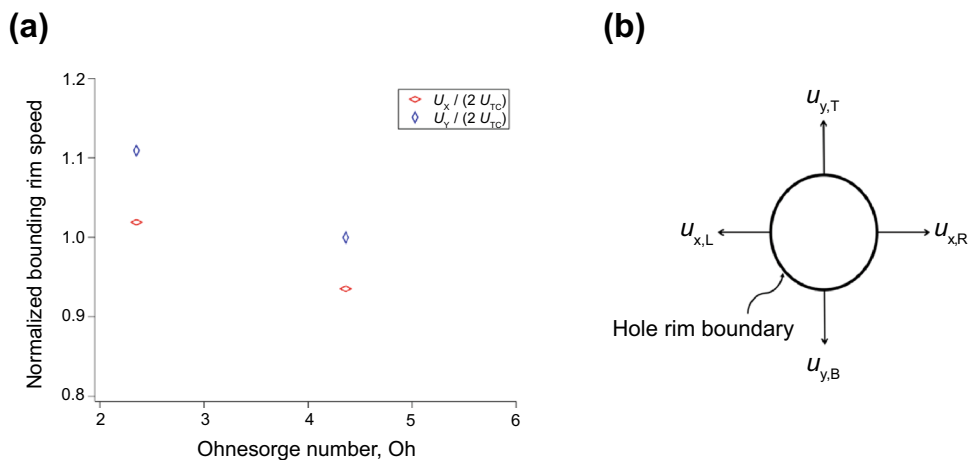
(a)
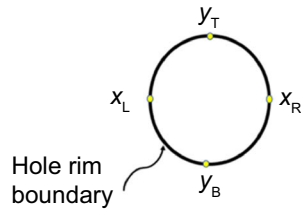
(b)
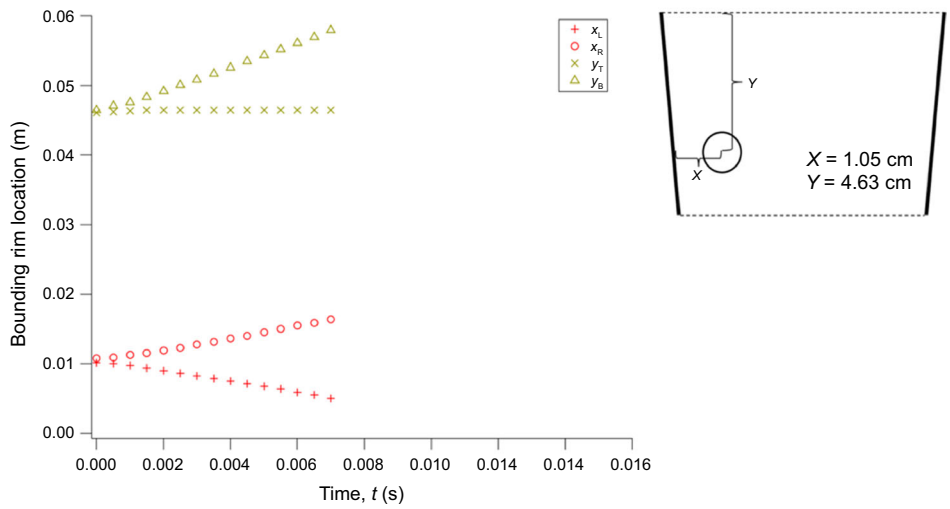
(c)

Fig. 7: (a) The schematics of bounding rims at different locations in the curtain. The dynamics of bounding rim in horizontal and vertical directions for (b) sample 2, (c) and sample 4

(a)   **(b)**

Fig. 8: (a) Normalized measured speeds of the bounding rim retraction in *x*-direction (i.e., $U_X/(2\ U_{TC}) = (u_{x,L} + u_{x,R})\ /\ (2\ U_{TC})$), and *y*-direction (i.e., $U_Y/(2\ U_{TC}) = (u_{y,B} + u_{y,T})/(2\ U_{TC})$) versus the Ohnesorge number, Oh, for two emulsion solutions. (b) Schematics of the location on the bounding rim where the speeds were measured

Table 2: The details of the curtain breakup for shear thinning solutions

Sample	X^* (cm)	Y^* (cm)	$u_{x,L}$ (m/s)	$u_{x,R}$ (m/s)	$u_{y,B}$ (m/s)	$u_{y,T}$ (m/s)	U_{TC} (m/s)	$U_{Curtain}$ (m/s)	Oh	t (μm)
2	1.05	4.63	0.75	0.84	1.67	0.03	0.85	0.75	4.36	102
4	1.82	3.71	0.80	0.79	1.72	0.01	0.78	0.78	2.35	174

*X: hole distance from the edge guide; Y: hole distance from exit of the die
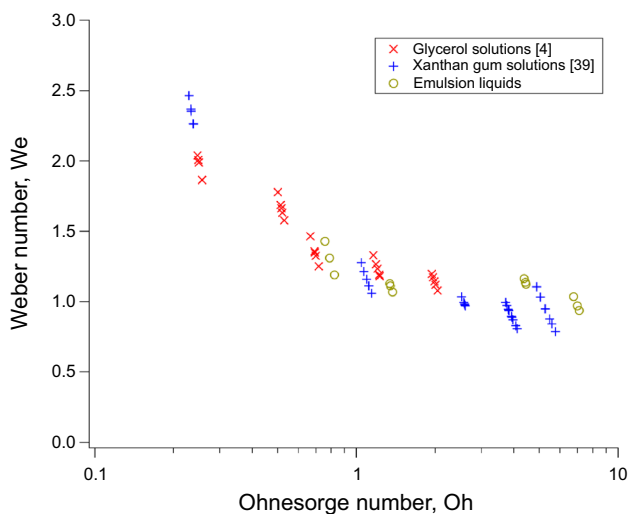
Fig. 9: Critical Weber number, We, at which the liquid curtain breaks as a function of the Ohnesorge number, Oh, for curtain stability of three liquid models, i.e., Newtonian liquids (glycerol solutions),[4] shear thinning liquids (xanthan gum solutions),[38] and emulsion liquids

Liquid curtain stability

The critical flow rate below which the curtain breaks was recorded for the different emulsion solutions. The critical flow rate represented by the Weber number (ratio of inertial and capillary forces) versus the Ohnesorge number, defined in terms of the characteristic dynamic viscosity, $\mu_{13.5}$, which is the dynamic viscosity at shear rate 13.5 (1/s), is shown in Fig. 9. The critical flow rate decreases as Ohnesorge number increases.

The critical Weber numbers reported in the previous studies[4,38] for the single-phase liquids (i.e., Newtonian liquids and xanthan gum solutions) are also included in Fig. 9. The behavior of the emulsion samples follows the general trend of the single-phase liquids (i.e., Newtonian and shear thinning) with the Oh defined in terms of the characteristic shear viscosity.

Surface tension is the major difference in the physical properties of the emulsion solutions. Figure 10 shows the minimum flow rate per unit width, Q_{min}, at which the emulsion liquid curtain breaks up as a function of the surface tension, σ. The results reveal that as surface tension increases, the liquid curtain becomes more unstable by breaking up the liquid curtain at larger flow rate. The minimum flow rate rises linearly as surface tension of the emulsion increases.
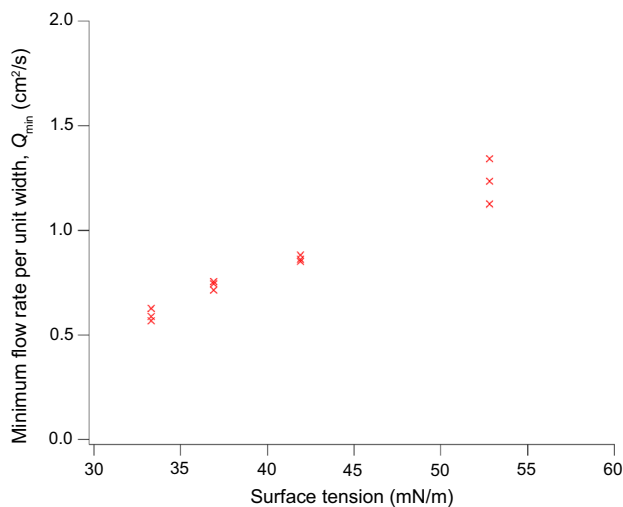
Stability of the dynamic contact line

In curtain coating, liquid experiences large shear rate near the dynamic contact line along the impingement zone. Hence, high-shear viscosity plays a significant role in determining onset of air entrainment.[39–42] The
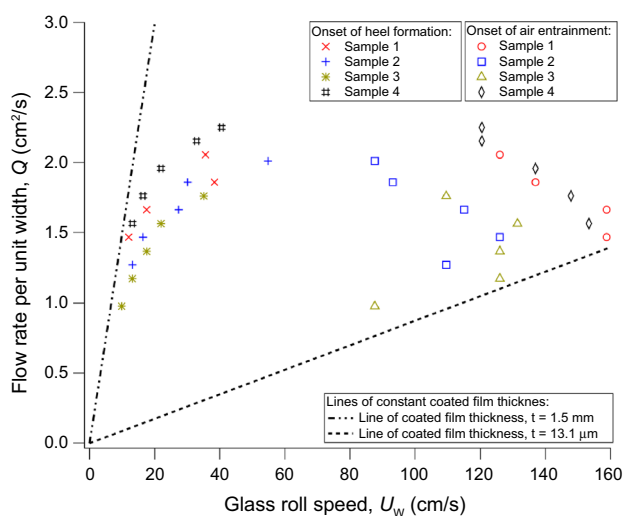
shear thinning behavior of emulsion solution leads shear viscosity to drop dramatically as shear rate increases. In addition to high shear viscosity, surface tension is an important factor to determine the critical condition at which the dynamic contact line becomes unstable.

At flow rates, higher than the minimum flow at which the curtain of emulsion solution is stable, the speeds, at which heel formation and air entrainment start to happen, were recorded accordingly as indicated in Fig. 11. Onset of heel formation is almost similar for emulsion solutions tested. This is because the shear viscosity curve and density are similar for emulsion solutions. However, onset of air entrainment is delayed as 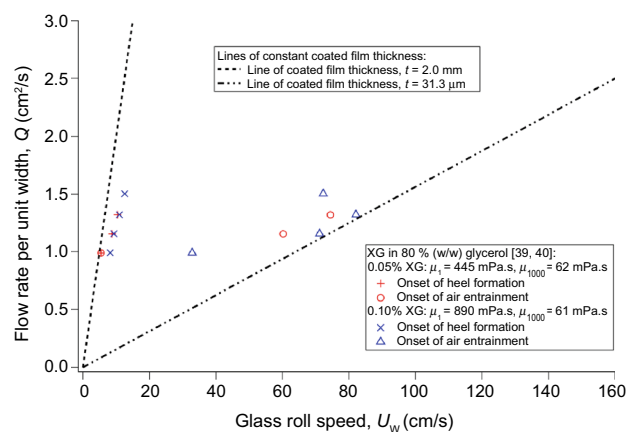surface tension increases. This is related to the fact that as surface tension rises, contact line speed, U_w, can increase to a much larger value before the capillary number, Ca, defined as $Ca = \frac{\mu U_w}{\sigma}$, reaches the maximum value where contact angle becomes 180°, where air pockets start to entrain. By considering the contact line velocity at the impingement zone, U, and the volumetric flow rate per unit width, Q, values at the maximum possible glass roller speeds for the four emulsion samples, and subsequently evaluating the thickness of the coated emulsion film, h_{film}, as well as the average shear rate in the viscous boundary layer of the impinging curtain according to $U/(h_{film})$ determines the shear rates in the range of 10,800–15,900 s^{-1}. These shear rates are near the point where the region of the shear viscosity curves of the shear thinning emulsion samples merges with the high-shear Newtonian plateau. As a result of these findings, the corresponding shear viscosities represent the high-shear viscosities of the four emulsions. Based on the range of the capillary numbers considered in this study (Ca ~ 1.1–1.9), which corresponds to the high-shear viscosities of the emulsion samples at the region of the liquid film impingement with the glass roller, this range of the capillary number indicates that effects of the capillary force as well as the viscous force are closely competing to influence the stability of the dynamic contact line at the impingement zone for determining the onset of the air entrainment. Therefore, emulsion samples 1 and 4, which promote the air entrainment at higher contact line velocities than emulsion samples 2 and 3, exhibit lower high-shear viscosities compared to the emulsions 2 and 3. In general, lower high-shear viscosities delay the onset of air entrainment, hence occurring at higher contact line speeds. Therefore, the difference in the air entrainment corresponding to the critical contact line speed between emulsion samples 1/4 and 2/3 could as well be explained by a difference in high-shear viscosity as well as the difference in surface tension.

Fig. 10: Minimum flow rate per unit width of the curtain, Q_{min}, as a function of the surface tension, σ, of the emulsion samples tested in this study

Fig. 11: Onsets of heel formation and air entrainment for curtain coating of emulsion solutions

Fig. 12: Onsets of heel formation and air entrainment for curtain coating of xanthan gum solutions in glycerol reported from previous study[39,40]

The results for onsets of heel formation and air entrainment of emulsion solutions were also compared with the results for single-phase shear thinning solutions [i.e., xanthan gum, XG, in glycerol (80 wt%)], as shown in Fig. 12. Emulsion sample 4 has similar high-shear viscosity and surface tension to those of xanthan gum in glycerol (80 wt%). However, the onset of air entrainment for the emulsion sample 4 started to happen at a much larger speed compared to the speeds at which the onset of air entrainment happened for xanthan gum solution. This can be related to the role of multiphase characteristic of the emulsion solution.

Conclusions

The effect of physical properties on emulsion curtain stability was studied experimentally by high-speed visualization of the sequence of events that ultimately led to the curtain breakup and by determining the critical flow rate below which the curtain becomes unstable. The velocity evolution along the curtain was measured at different distances from the edges. It was found that the formed viscous boundary layer along the edge guide causes the curtain velocity to deviate from the free fall velocity.

Previous analyses[11,13] proposed a simple criterion for curtain stability based on the ratio of the curtain velocity, which moves any hole in the curtain downward, to the rim retraction speed, which opens the hole. If the ratio is above one, the curtain is stable. The high-speed visualization images presented here confirm this hypothesis. At larger flow rate, a hole is convected down the curtain before it becomes large enough to cause the curtain breakup. Below a critical flow rate, at which the retraction speed is larger than the curtain speed, the hole grows, leading to the curtain breakup.

The results show that the dynamics of the curtain breakup is governed by the characteristic dynamic viscosity, μ_C, determined by the shear rate related to the expansion speed, u_{rim}, of the hole formed within in the emulsion curtain ($\mu_C = \mu(u_{rim}/L)$), and the surface tension of the emulsion liquid. Higher characteristic dynamic viscosity as well as lower surface tension leads to a more stable curtain (i.e., lower critical flow rate), hence thinner emulsion liquid film on the substrate being coated. However, it is important to note that at such very low flow rates (i.e., less than 0.8 cm^2/s), the substrate can usually not be coated, especially at the substrate speeds which are the interest of the industrial applications, due to the fact that the air entrainment occurs at very low substrate speeds.

The dependence of the critical Weber number below which the curtain breaks as a function of the Ohnesorge number, Oh, follows the general behavior previously reported for the single-phase shear thinning and Newtonian liquids[4,38] when the Ohnesorge number, Oh, is determined by the characteristic dynamic viscosity (Oh $= \frac{\mu_C}{\sqrt{2\rho\sigma t}}$).

The effect of physical properties of emulsion liquids on stability of the dynamic contact line in curtain coating was also studied via high-speed visualization of the dynamic contact line at the impingement zone of the liquid curtain with the glass roller. The critical conditions at which the dynamic contact line becomes unstable were determined by the onset of the air entrainment and the heel formation. The surface tension shows a strong stabilizing effect on the dynamic contact line delaying onset of the air entrainment over the range of the speeds the curtain coating experiments were conducted. Our finding shows that the surface tension increase in emulsion liquid films leads to faster curtain coating of the substrates but with thicker liquid film.

References

1. Miyamoto, K, Katagiri, K, "Curtain Coating." In: Kistler, SF, Schweizer, PM (eds.) *Liquid Film Coating: Scientific Principles and Their Technological Implications.* (1997)
2. Blake, TD, Clarke, A, Ruschak, KJ, "Hydrodynamic Assist of Dynamic Wetting." *AIChE J.*, **40** 229–242 (1994)
3. Marston, JO, Simmons, MJH, Decent, SP, "Influence of Viscosity and Impingement Speed on Intense Hydrodynamic Assist in Curtain Coating." *Exp. Fluids*, **42** 483–488 (2007)
4. Mohammad Karim, A, Suszynski, WJ, Francis, LF, Carvalho, MS, "Effect of Viscosity on Liquid Curtain Stability." *AIChE J.*, **64** 1448–1457 (2018)
5. Mohammad Karim, A, Suszynski, WJ, Pujari, S, Francis, LF, Carvalho, MS, "Delaying Breakup and Avoiding Air Entrainment in Curtain Coating Using a Two-Layer Liquid Structure." *Chem. Eng. Sci.*, **213** 115376 (2020)
6. Mohammad Karim A, Suszynski, WJ, Griffith, WB, Pujari, S, Carvalho, MS, Francis, LF, "Effect of Rheological Properties on Liquid Curtain Coating." In: 70th Annual Meeting of the Fluid Dynamics Division of the American Physical Society, 62(14), Denver, CO, 2017
7. Mohammad Karim, A, Suszynski, WJ, Griffith, WB, Pujari, S, Carvalho, MS, Francis, LF, "Effect of Elasticity on Stability of Viscoelastic Liquid Curtain." In: AIChE Annual Meeting, Minneapolis, MN, 2017
8. Mohammad Karim, A, Suszynski, WJ, Griffith, WB, Pujari, S, Francis, LF, Carvalho, MS, "Effect of Viscoelasticity on Stability of Liquid Curtain." *J. Non-Newtonian Fluid Mech.*, **257** 83–94 (2018)
9. Mohammad Karim, A, Suszynski, WJ, Francis, LF, Carvalho, MS, "Effect of Elasticity on Stability of Viscoelastic Liquid Curtain." In: 69th Annual Meeting of the Fluid Dynamics

Division of the American Physical Society, 61(2), Portland, OR, 2016

10. Mohammad Karim, A, Suszynski, WJ, Griffith, WB, Pujari, S, Francis, LF, Carvalho, MS, "Effect of Viscoelasticity on Stability of Curtain Coating." In 19th International Society of Coating Science and Technology Symposium (ISCST). Long Beach, CA, 2018

11. Taylor, GI, "The Dynamics of Thin Sheets of Fluid. III. Disintegration of Fluid Sheets." *Proc. R. Soc. Lond. A*, **253** 313–321 (1959)

12. Brown, DR, "A Study of the Behaviour of a Thin Sheet of Moving Liquid." *J. Fluid Mech.*, **10** 297–305 (1961)

13. Lin, SP, Roberts, G, "Waves in a Viscous Liquid Curtain." *J. Fluid Mech.*, **112** 443–458 (1981)

14. Lin, SP, "Stability of a Viscous Liquid Curtain." *J. Fluid Mech.*, **104** 111–118 (1981)

15. Lin, SP, Lian, ZW, Creighton, BJ, "Absolute and Convective Instability of a Liquid Sheet." *J. Fluid Mech.*, **220** 673–689 (1990)

16. Finnicum, DS, Weinstein, SJ, Ruschak, KJ, "The Effect of Applied Pressure on the Shape of a Two-Dimensional Liquid Curtain Falling Under the Influence of Gravity." *J. Fluid Mech.*, **255** 647–665 (1993)

17. De Luca, L, Meola, C, "Surfactant Effects on the Dynamics of a Thin Liquid Sheet." *J. Fluid Mech.*, **300** 71–85 (1995)

18. Roche, JS, Le Grand, N, Brunet, P, Lebon, L, Limat, L, "Perturbations on a Liquid Curtain Near Break-Up: Wakes and Free Edges." *Phys. Fluids*, **18** 082101 (2006)

19. Becerra, M, Carvalho, MS, "Stability of Viscoelastic Liquid Curtain." *Chem. Eng. Process.*, **50** 445–449 (2011)

20. Sünderhauf, G, Raszillier, H, Durst, F, "The Retraction of the Edge of a Planar Liquid Sheet." *Phys. Fluids*, **14** 198–208 (2002)

21. Savva, N, Bush, JWM, "Viscous Sheet Retraction." *J. Fluid Mech.*, **626** 211–240 (2009)

22. Burley, R, Kennedy, BS, "An Experimental Study of Air Entrainment at a Solid/Liquid/Gas Interface." *Chem. Eng. Sci.*, **31** (10) 901–911 (1976)

23. Blake, TD, Ruschak, KJ, "A Maximum Speed of Wetting." *Nature*, **282** 489–491 (1979)

24. Vandre, E, Carvalho, MS, Kumar, S, "Characteristics of Air Entrainment During Dynamic Wetting Failure Along a Planar Substrate." *J. Fluid. Mech.*, **747** 119–140 (2014)

25. Weinstein, SJ, Ruschak, KJ, "Coating Flows." *Annu. Rev. Fluid Mech.*, **36** (1) 29–53 (2004)

26. Blake, TD, Bracke, M, Shikhmurzaev, YD, "Experimental Evidence of Nonlocal Hydrodynamic Influence on the Dynamic Contact Angle." *Phys. Fluids*, **11** (8) (1999)

27. Yamamura, M, "Assisted Dynamic Wetting in Liquid Coatings." *Colloids Surf. A*, **311** 55–60 (2007)

28. Marston, JO, Simmons, MJH, Decent, SP, Kirk, SP, "Influence of the Flow Field in Curtain Coating onto Pre-wet Substrates." *Phys. Fluids*, **18** 112102 (2006)

29. Blake, TD, Dobson, RA, Ruschak, KJ, "Wetting at High Capillary Numbers." *J. Colloid Interface Sci.*, **279** 198–205 (2004)

30. Yamamura, M, Suematsu, S, Kajiwara, T, Adachi, K, "Experimental Investigation of Air Entrainment in a Vertical Liquid Jet Flowing Down onto a Rotating Roll." *Chem. Eng. Sci.*, **55** (5) 931–942 (2000)

31. Liu, CY, Vandre, E, Carvalho, MS, Kumar, S, "Dynamic Wetting Failure in Surfactant Solutions." *J. Fluid Mech.*, **789** 285–309 (2016)

32. Choi, EH, Kim, CH, Youn, HJ, Lee, HL, "Influence of PVA and CMC on the Properties of Pigment Coating Colors and Their Effects on Curtain Stability." *BioResources*, **10** (4) 7188–7202 (2015)

33. Mohammad Karim, A, Kavehpour, HP, "Effect of Viscous Force on Dynamic Contact Angle Measurement Using Wilhelmy Plate Method." *Colloids Surf. A*, **548** 54–60 (2018)

34. Weinstein, SJ, "Wave Propagation in the Flow of Shear-Thinning Fluids Down an Incline." *AIChE J.*, **36** 1873–1889 (1990)

35. Jiang, WY, Helenbrook, BT, Lin, SP, Weinstein, SJ, "Low-Reynolds-Number Instabilities in Three-Layer Flow Down an Inclined Wall." *J. Fluid Mech.*, **539** 387–416 (2005)

36. Marston, JO, Thoroddsen, ST, Thompson, J, Blyth, MG, Henry, D, Uddin, J, "Experimental Investigation of Hysteresis in the Break-Up of Liquid Curtains." *Chem. Eng. Sci.*, **117** 248–263 (2014)

37. Culick, FEC, "Comments on a Ruptured Soap Film." *J. Appl. Phys.*, **31** 1128–1129 (1960)

38. Mohammad Karim, A, Suszynski, WJ, Griffith, WB, Pujari, S, Francis, LF, Carvalho, MS, "Effect of Rheological Properties of Shear Thinning Liquids on Curtain Stability." *J. Non-Newtonian Fluid Mech.*, **263** 69–76 (2019)

39. Francis, LF, Mohammad Karim, A, Suszynski, WJ, Pujari, S, Carvalho, MS, "Effect of Rheology on Curtain Coating." In: Industrial Partnership for Research in Interfacial and Materials Engineering (IPRIME) Annual Meeting, Minneapolis, MN, 2019

40. Mohammad Karim, A, Suszynski, WJ, Griffith, WB, Pujari, S, Carvalho, MS, Francis, LF, "Effect of Rheological Properties on Liquid Curtain Coating." In: Industrial Partnership for Research in Interfacial and Materials Engineering (IPRIME) Annual Meeting, Minneapolis, MN, 2017

41. Mohammad Karim, A, Suszynski, WJ, Pujari, S, Francis, LF, Carvalho, MS, "Using Two-Layer Structure to Expand Operability Window of Curtain Coating Process." In: 20th International Society of Coating Science and Technology Symposium (ISCST), Virtual Event, 2020

42. Mohammad Karim, A, "Parametric Study of Liquid Contact Line Dynamics: Adhesion vs. Hydrodynamics" Ph.D. Thesis, UCLA, 2015